Available online at www.sciencedirect.com
SCIENCE DIRECT
Biochemical Pharmacology 70 (2005) 287–299
Biochemical Pharmacology
www.elsevier.com/locate/biochempharm

Tangutorine induces p21 expression and abnormal mitosis in human colon cancer HT-29 cells

B.P.L. Liu [a], E.Y.Y. Chong [a], F.W.K. Cheung [a], Jin-Ao Duan [b], Chun-Tao Che [c], W.K. Liu [a,*]

[a] *Department of Anatomy, Faculty of Medicine, The Chinese University of Hong Kong, Shatin, New Territories, Hong Kong, PR China*
[b] *Academy of Chinese Medicine of Jiangsu Province, Nanjing, PR China*
[c] *School of Chinese Medicine, The Chinese University of Hong Kong, Shatin, New Territories, Hong Kong, PR China*

Received 9 March 2005; accepted 21 April 2005

Abstract

A novel β-carboline alkaloid, tangutorine (benz[*f*]indolo[2,3-*a*]quinolizidine) was isolated from the leaves of *Nitraria tangutorum* L. [Duan JA, Williams ID, Che CT, Zhou RH, Zhao RH, Tangutorine: a novel β-carboline alkaloid from *Nitraria tangutorum*. Tetrahedron Lett 1999;40:2593–6], and its unique structural characters led us to initiate a study of its potential anti-proliferation activity. The in vitro treatment with low doses of tangutorine slightly stimulated the proliferation of human colon cancer HT29 cells until at concentrations higher than 6.25 μg/ml when the cell numbers, cellular MTT reduction, and cell proliferation by ^{3}H-thymidine incorporation decreased in a dose-dependent manner (IC_{50} = 15 μg/ml = 48 μM). Morphological studies of cells by fluorescence and electron microscopy did not show features for apoptosis but only large vacuoles, swollen mitochondria and dense cytoskeletal filaments bunching in the cytoplasm. Immunoblotting analysis revealed a dramatic induction of cyclin kinase inhibitor p21 as well as an inhibition of topoisomerase II expression at 25 μg/ml tangutorine, thereby impeding cell progression from S to G2/M phase. Cells accumulated at G1 phase of the cell cycle at concentrations ≥50 μg/ml tangutorine. Interestingly, some cells escaped from prolonged growth arrest without cell division and resulted in binucleated and polyploid G1 cells. Taken all results together, tangutorine induced a p21 suppression of all cyclins and their associated kinases, such as the topoisomerase II, and thus inhibited normal DNA replication and mitosis.

Keywords: Tangutorine; Cyclin kinase inhibitor p21; HT29 cells; Growth arrest; Abnormal mitosis

1. Introduction

Colorectal cancer is the third most common form of malignancy in both men and women around the world. Alarmingly increasing numbers of reported cases of colon cancer in recent years has made this form of cancer a major health concern, 57,100 deaths alone in the United States in 2003 and an estimate of 147,500 new cases in the coming year [2]. The mortality statistics for the leading causes of cancer deaths lists colon and rectum cancer at 10% for both genders in the United States [2]. The most recent statistics from Hong Kong also listed colorectal cancer as the third most common cancer in Hong Kong. The Hong Kong Cancer Registry also found similar statistics from the United States that colon cancer is the third leading cause of cancer mortality in Hong Kong [3].

Aside from surgery and radiotherapy, chemotherapy is one of the most common forms of treatment used as therapy for colon cancer. Current chemotherapeutic agents used in treating colon cancer include virulent drugs such as fluorouracil (5-FU), oxaliplatin, CPT-11 (irinotecan), and non-steroidal anti-inflammatory drugs (NSAIDs) [4–7]. Most of these antineoplastic agents directly inhibit DNA synthesis, the mitotic apparatus, or topoisomerases, leading to a cascade of events that affect the proliferation, differentiation, and apoptotic properties of the cancer cells. Since cancer cells lack the normal growth controls including a loss of differentiation, self-sufficiency in growth signals, the ability to evade programmed cell death, and an unlimited replicative potential [8], it is not surprising that the majority of cytotoxic agents used in combating cancer are aimed at reversing these aberrant characteristics of carcinomas. Current issues in cancer research involve searching for novel anticancer compounds that can be used to regulate the cell cycle and lead to more effective treatments of tumors.

* Corresponding author. Tel.: +852 2609 6896; fax: +852 2603 5031.
E-mail address: ken-liu@cuhk.edu.hk (W.K. Liu).

0006-2952/$ – see front matter © 2005 Elsevier Inc. All rights reserved.
doi:10.1016/j.bcp.2005.04.024

There are 15 species of *Nitraria* plants growing on saline plains of Asia, the Middle East, and Northern Africa [9]. Plants of this genus are known to contain indoloquinolizidine alkaloids including quinazolines, quinolizidines, and spiropiperdines. A novel β-carboline alkaloid, tangutorine, was isolated from the leaves of *Nitraria tangutorum* L. [1], as the only natural compound to contain a benz[*f*]-indolo[2,3-*a*]quinolizidine unit in the family of indole alkaloids. The synthesis of the tangutorine skeleton [10] and total synthesis of (±)-tangutorine [11,12] have been accomplished. Structurally, tangutorine is related to monoterpenoid indole alkaloids like (+)-deplancheine [13] and (+)-geissoschizine [14], all derived biosynthetically from the amino acid tryptophan [11].

In vitro studies have shown the ability of many β-carbolines such as camptothecin, etoposide, harmine, adriamycin and manzamine to derail the cell cycle progression of tumor cells, such as a G2 cell cycle arrest, aberrant mitosis and cell death in tumor cells [15–18]. Studies have also shown harmine to induce DNA damage [19] and cause specific inhibition of proteins involved in cell cycle regulation of carcinoma cell lines [20]. The spindle disorganization and chromosome missegregation in cancer cells are also considered toxic mechanisms of some potential anticancer β-carboline drugs [18].

Although no information is available concerning the biological effects of tangutorine, it was hypothesized that possessing a cyclic alkaloid similar to harmine, tangutorine can disrupt the proliferative state of cancer cells and block the activity of topoisomerases. Preliminary studies have indeed shown that tangutorine is a topoisomerase II inhibitor in prostate cancer LNCaP cells (unpublished data). In this study, a battery of experiments was carried out to explore the cytotoxicity of tangutorine on HT29 cells to show effects on the regulation of cell cycle and cellular morphology.

2. Materials and methods

2.1. Tested compound

Tangutorine was isolated from the leaves of *Nitraria tangutorum* and the structure was determined on the basis of spectral and X-ray crystallographic data (Fig. 1) [1]. The compound possesses a novel β-carboline skeleton and has a molecular weight of 308, and it was dissolved in DMSO at a concentration of 160 mM, which was then diluted to appropriate concentrations with culture medium and used before each experiment. The final concentration of DMSO did not exceed 0.5% in any experiment.

2.2. Cell culture and synchronization

Human colon carcinoma HT29 cell line (HTB-38, ATCC, Rockville, MD, USA) was propagated in RPMI-1640 medium (Life Technologies, Inc., NY, USA) supplemented with 10% FBS (Life Technologies, Inc., NY, USA), 2 mM L-glutamine (Sigma, St. Louis, MO, USA), 100 IU/ml penicillin (Sigma, St. Louis, MO, USA), and 100 μg/ml streptomycin sulfate (Life Technologies, Inc., NY, USA). Cells were incubated in a humidified atmosphere of 5% CO_2 at 37 °C. For experiments, HT29 cells were seeded at subconfluent densities and left to adhere for 24 h. Cell synchronization in G0/G1 phase of the cell cycle at 80% (Fig. 6) was induced by serum starvation for 24 h [21] and supplemented RPMI was then added to resume the cell cycle. Close monitoring of the HT29 cells after release back into the cell cycle showed 0–14, 15–18, and 19–27 h for G1, S and G2/M phases, respectively (data not shown).

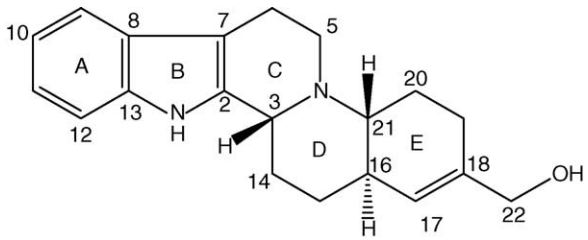

Fig. 1. Chemical structure of tangutorine.

2.3. Growth assay

Synchronized HT29 cells (2×10^5 cells/ml/well) were treated with tangutorine at different concentrations in 24-well culture plates for 24 and 48 h before the cells were detached with 0.25% trypsin–EDTA for determination of cell viability using the trypan blue exclusion method. Cells (1×10^4 cells/0.1 ml/well) were incubated with a serial concentrations of tangutorine in 96-well plates for 24 and 48 h before the cultures were subjected to either MTT (3-4,5-dimethylthiazol-2-yl-2,5-diphenyltetrazolium bromide) assay or ^{3}H-thymidine (^{3}H-Tdr) incorporation assay as described in a previous paper [22]. All reported values are the means of triplicate samples.

2.4. Fluorescence staining for morphological observation

HT29 cells were seeded on gelatin-coated coverslips and treated with different concentrations of tangutorine for 24 h before they were washed with D-PBS and fixed with 70% cold ethanol for 5 min. The cells were then stained with 0.01% acridine orange in 0.06 M phosphate buffer (pH 6.0) and differentiated with 0.1 M calcium chloride (Sigma, St. Louis, MO, USA). Images of the cells were captured using a fluorescence microscope (Axioskop, Zeiss, Germany) with a 520 nm barrier filter and 450–490 nm excitation block filter [23].

2.5. Electron microscopy

Cells were seeded overnight onto coverslips and treated with tangutorine for 24 and 48 h. Immediately after removal of medium containing the drugs cells were rinsed with PBS and fixed with 2.5% glutaraldehyde at 4 °C, rinsed with 0.1 M phosphate buffer, pH 7.4 and post-fixed in 1% aqueous osmium tetroxide for 30 min. After washing with 0.1 M phosphate buffer, the samples were dehydrated through graded ethanol concentrations (70, 85, 95, and 100% ethanol), and one portion of the cells were subjected to critical point dried with liquid carbon dioxide using a Critical Point Dryer (LADD Research Industries, Burlington, VT, USA), coated with gold palladium carbon, and the surface morphology was observed using a JSM-6301F scanning microscope (JEOL, Japan) [22]. Another portion of cells were embedded in Spurr's medium. Sections were cut with an Ultracut R (Leica, Austria), double-stained with uranyl acetate and lead citrate, and examined with a Hitachi 7100FA transmission electron microscope (Japan). Kodak Electron Microscope Film, (EStar Thick Base 4489, Eastman Kodak Company, Rochester, NY, USA) was used for transmission electron microphotographs [23].

2.6. Flow cytometry for cell cycle analysis

For analysis of the cell cycle of treated cells, 1×10^6 cells were fixed with 70% ethanol overnight at 4 °C. Cells were then washed with Dulbecco's Phosphate-Buffered Saline (D-PBS, Life Technologies, Inc., Grand Island, NY, USA) twice and incubated with 1 ml of propidium iodide solution (1 mg/ml PI), 2% RNase A, and 1% Triton X-100 (Sigma, St. Louis, MO, USA) at room temperature for 30 min. PI-intercalated cells were measured with an argon laser at 488 nm using a Beckman Coulter EPICS Altra Flow Cytometer, (Beckman Coulter, Inc., Miami, FL, USA). Approximately 10,000 cells were analyzed per sample, and the results were analyzed using Expo32 software (Beckman Coulter, Inc., USA) [23].

2.7. Reverse transcription-polymerase chain reaction analysis (RT-PCR)

HT29 cells (5×10^6 cells) were treated with a serial concentrations of tangutorine for various time points, ranging from 2, 4, 8, and 16 h before their total cellular RNA was isolated with TRIzol® Reagent (Invitrogen Life Technologies, Carlsbad, CA, USA), reverse-transcribed at 42 °C for 50 min using a SuperScript™ III Reverse Transcriptase Kit (Invitrogen Life Technologies, Carlsbad, CA, USA), and each RT product was subjected to PCR using Thermoprime DNA polymerase (GIBCO/BRL, N.Y. USA) and primers for cyclin kinase inhibitor p21 (forward 5′-CTTTGACTTCGTCACGGAGAC-3′ and reverse 5′-AGGCAGCGTATATCAGGAGAC-3′) (GIBCO/BRL) in a 9700 Perkin-Elmer thermocycler. The PCR products were separated on a 1.2% agarose gel and the relative intensity against respective β-actin was measured by a densitometer with Image Quant software (Personal Densitometer, Molecular Dynamics, USA) [24].

2.8. Western blot analysis

Treated cells were rinsed twice with PBS before Tris cell lysis buffer (50 mM Tris–Cl, 150 mM NaCl, 0.2% triton X-100, 10 μg/ml aprotinin, 0.5 mM PMSF) was added for the preparation of total cell lysate. Approximately 30 μg of total cellular proteins were separated on a 12% SDS-polyacrylamide gel which was then electrotransferred onto polyvinylidene difluoride (PVDF) blotting membranes (Roche Diagnostics Corporation, Indianapolis, IN, USA) using the semi-dry method. Membranes with equal amounts of protein per lane were incubated overnight with: antibodies against cell cycle regulatory proteins, cyclin D (sc-8396), cdk 4 (06-139), cyclin B (sc-752), cdc2(sc-54), cdc25C (sc-327), topoisomerase II (M7186), p21 (sc-6246), and PCNA (sc-56). All antibodies, except toposiomerase II (M7186 Dako Cytomation, Glostrup, Denmark) and cdk 4 (06-139, Upstate Biotechnology Inc., Lake Placid, NY, USA), were purchased from Santa Cruz Biotechnology, (Santa Cruz, CA, USA). After three rinses with TBS-T, the blots were incubated with horseradish peroxidase-conjugated (HRP) polyclonal goat anti-mouse or polyclonal goat-anti-rabbit IgG–HRP affinity isolated antibodies (Santa Cruz Biotechnology and Dako Cytomation) in TBS-T buffer. The signals were detected using the ECL™ Western Blotting Analysis System (Amersham Pharmacia Biotech, Piscataway, NJ, USA), followed by short exposures to Lumi-film Chemiluminescent Detection Film (Roche Diagnostics Corporation, Indianapolis, IN, USA). Antibodies were stripped by the Re-Blot Plus Western Blot Recycling Kit (Chemicon International, Inc., Temecula, CA, USA) and re-probed with other antibodies described as above. Band intensities were quantified by the software PD Quest (BioRad Laboratories, Hercules, CA, USA) and normalized by β-actin [25].

3. Results

3.1. Cytotoxicity assay

The MTT reduction is a common assay for evaluation of cell metabolism and viability, and was used to assess the cytotoxicity of tangutorine. An increase of cell metabolism and viability was demonstrated at doses $\leq$6.25 μg/ml, followed by a dose- and time-dependent decrease of MTT reduction activity after treatment with tangutorine from 6.25 to 200 μg/ml (Fig. 2a). IC_{50} values decrease depending on the exposure period to tangutorine, with values of 80 μg/ml (24 h) and 15 μg/ml (48 h). The potency of cytotoxicity on HT29 cells was not as dramatic

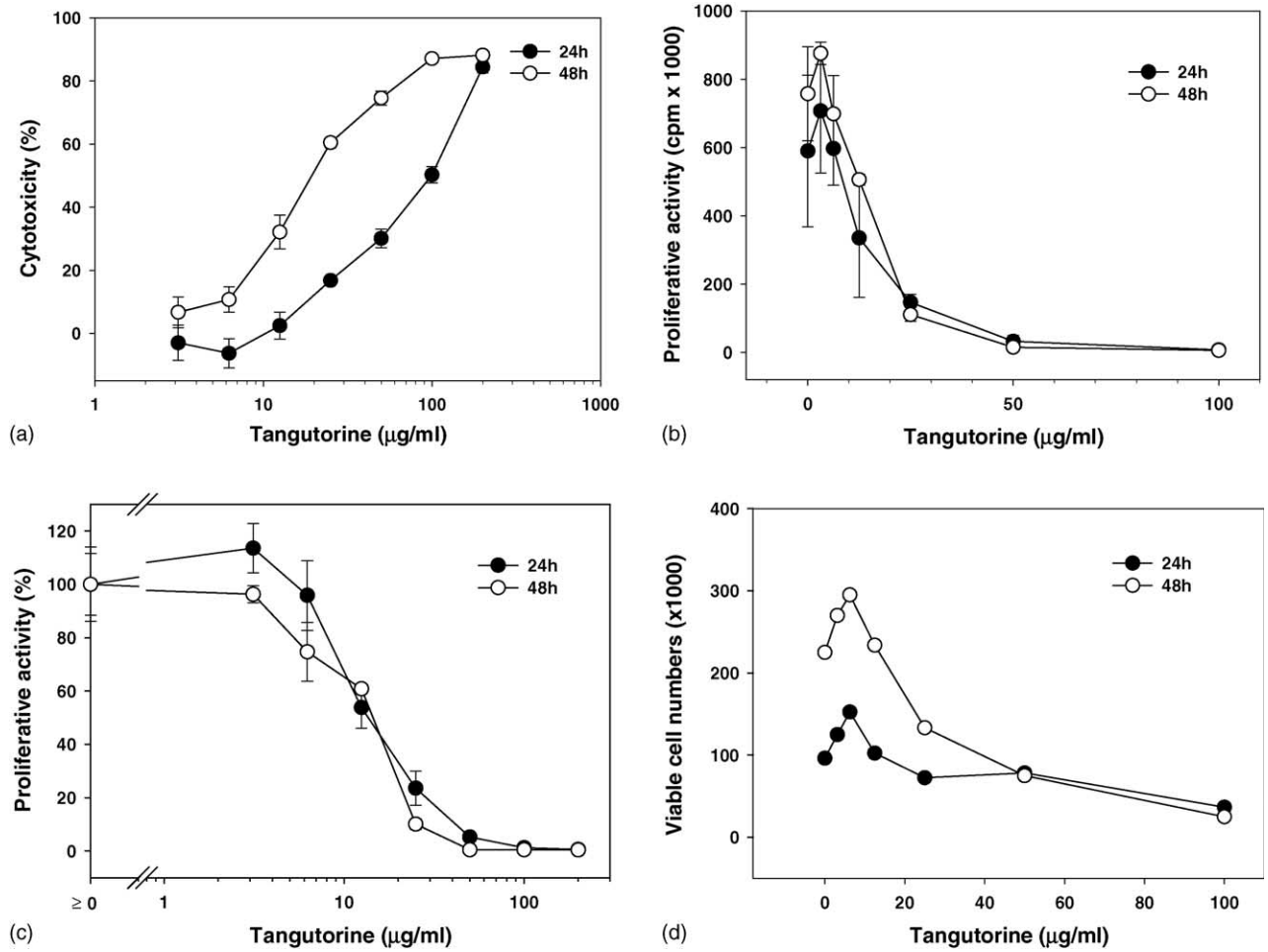

Fig. 2. Cytotoxicity of tangutorine on HT29 cells as determined by MTT assay (a); ^{3}H-thymidine incorporation assays (total incorporation counts (b) and percentage of untreated controls (c)), and trypan blue exclusion analysis (d) for 24 and 48 h.

at concentrations below 12.5 μg/ml for both time periods, but it is evident that the cytotoxicity of tangutorine on HT29 cells increased at both dose- and time-dependent manners.

Different patterns were observed between MTT cytotoxicity assay and ^{3}H-Tdr incorporation in the cytotoxicity evaluation of tangutorine in HT29 cells for 24 and 48 h. Results in Fig. 2b and c show up to 20% increase in both total and percent cellular ^{3}H-Tdr incorporation, respectively, at low concentrations of tangutorine ($\leq$6.25 μg/ml), but modest inhibition at concentrations between 6.25 and 12.5 μg/ml. The sharpest decreases in DNA synthesis occur at doses >12.5 μg/ml and there was little or no cellular uptake of ^{3}H-Tdr at concentrations over 50 μg/ml. The concentration of tangutorine used to reduce half of ^{3}H-Tdr incorporation (IC_{50}) was at around 15 μg/ml in both 24 and 48 h experiments, suggesting most of the cells would have lost their proliferative activity and had limited DNA replication after one cell cycle (24–48 h).

The results on cell count by trypan blue exclusion assay agreed with those of MTT assay and ^{3}H-Tdr incorporation experiment in that $\leq$6.25 μg/ml tangutorine could stimulate, although not statistically significant ($p > 0.05$), cell proliferation in a time-dependent manner with a decline of cell number thereafter (Fig. 2b).

3.2. Cell morphological cytotoxicity

Untreated HT29 cells grew in a monolayer, island-like manner that did not change even after treatment with tangutorine as shown in Fig. 3a and b. The presence of apoptotic bodies in the nucleus is a typical apoptotic marker [24], but HT29 cells stained with acridine orange did not show any sign of apoptotic bodies, regardless of the tangutorine dosage used (untreated, 25, 50 and 100 μg/ml for Fig. 3b, d, f and h, respectively). The amount of cytoplasmic vacuolation, however, increased in a dose- and time-dependent manner (Fig. 3h).

Exposure of HT29 cells to 25, 50, and 100 μg/ml of tangutorine for 24 h induced morphological changes that involved the microvilli, shape, and organelles of the cells as shown in Fig. 4. The most noticeable morphological structures on untreated and elongated HT29 cells (Fig. 4a) are the slender microvilli, also known as a brush border,

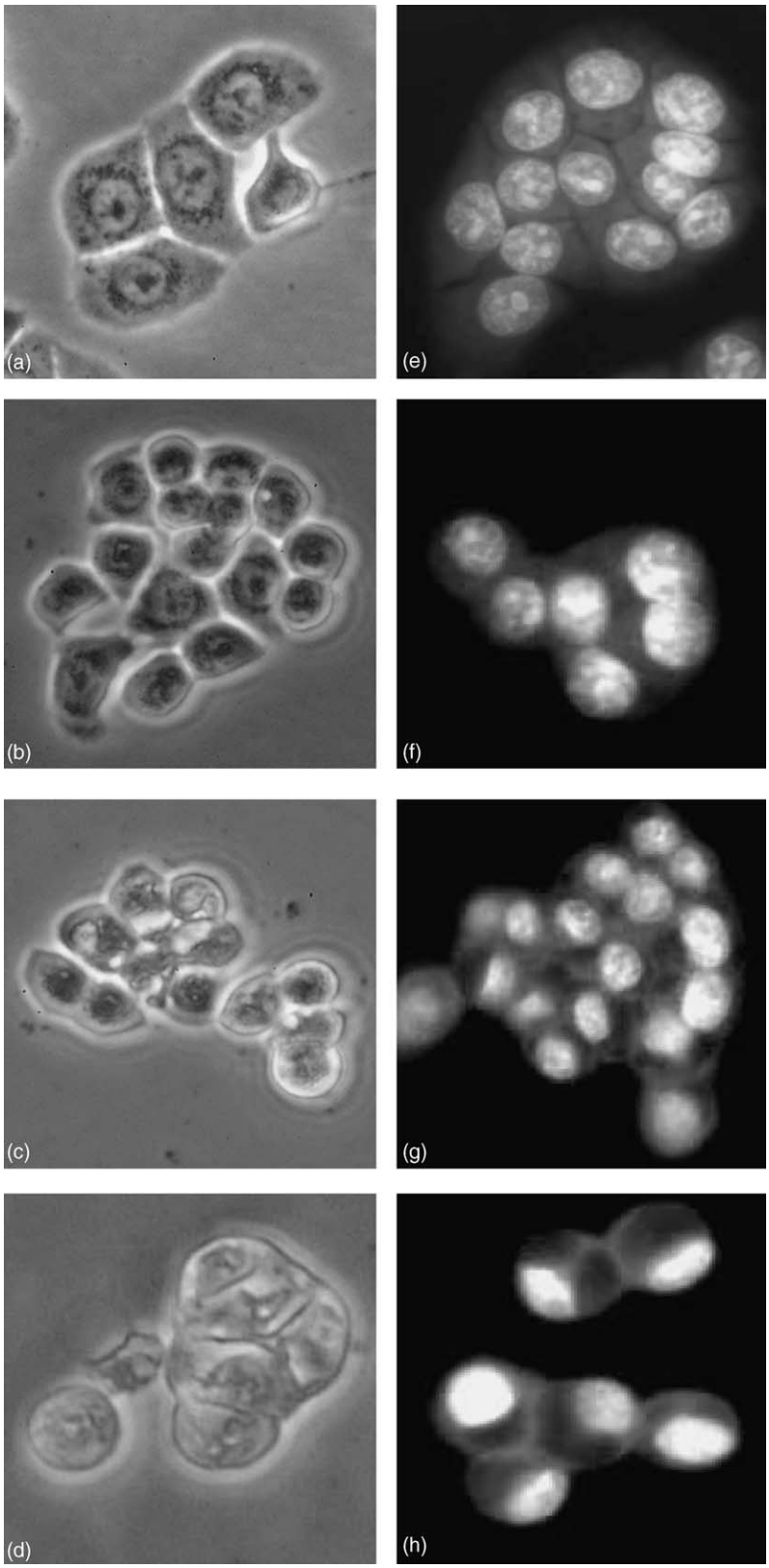

Fig. 3. Morphological changes of untreated HT29 cells (a and b) and cells treated with various doses of tangutorine untreated (a and b), 25 (c and d), 50 (e and f) and 100 μg/ml (g and h) for 24 h, as determined by phase contrast microscopy (a, c, e and g) and fluorescence microscopy for cells stained with acridine orange (b, d, f and h). Vaucolation in cytoplasm but no apoptotic bodies were common features of tangutorine-treated cells (400×).

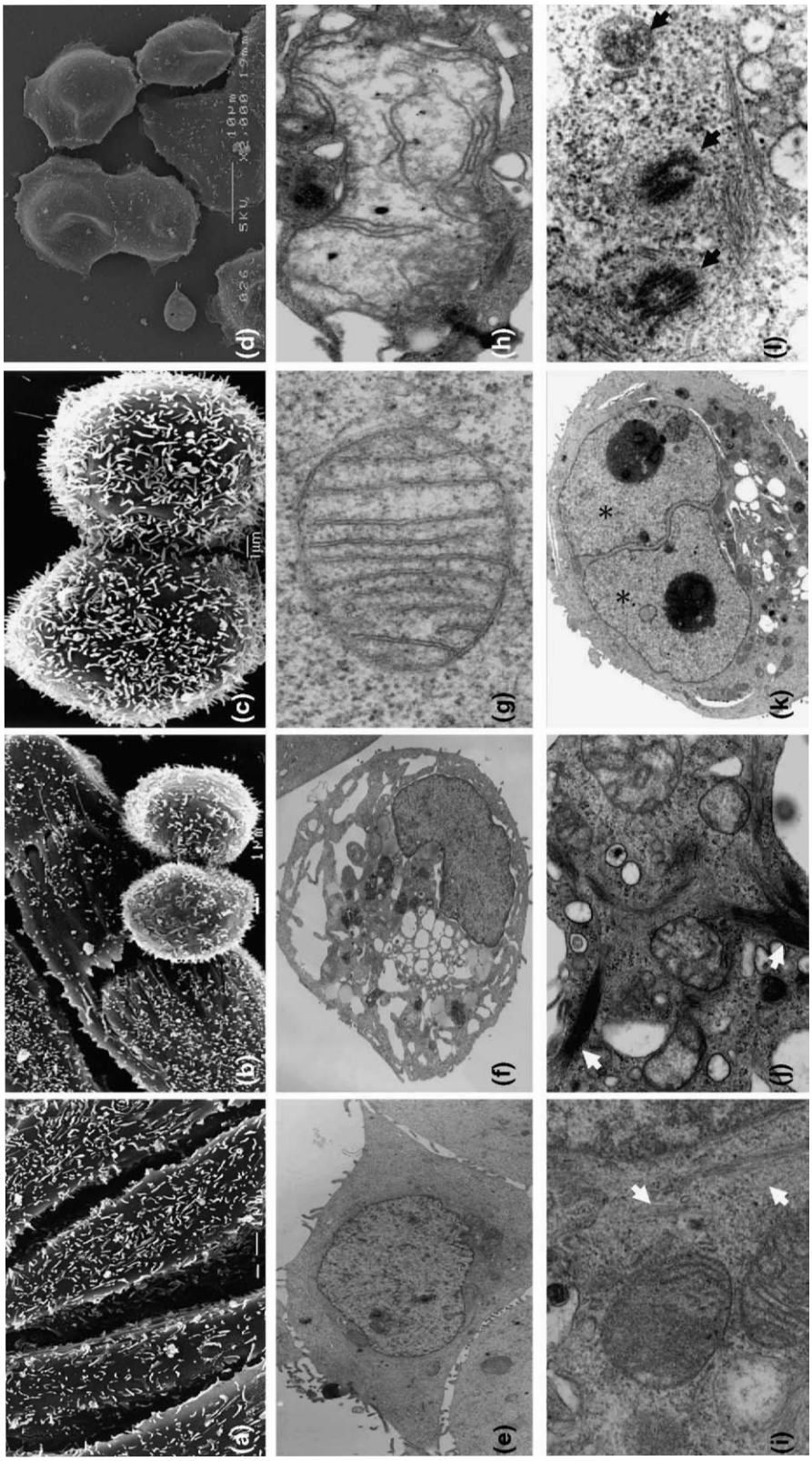

Fig. 4. Scanning electron micrographs showing microvilli on cell surface (a) and mitotic cells (c) were commonly observed in elongated untreated HT29 cells. The amount of microvilli decreased (b) to disappeared (d) in cells treated with 25–100 μg/ml tangutorine for 24 h. Centrally located nucleus (e, 3500×), intact mitochondria with shelf-like cristae (g, 50,000×), and cytoskeletal filaments (i, 30,000×) distributed in the cytoplasm of untreated cells, while numerous vacuoles with various sizes, swollen mitochondria with distorted cristae (h, 19,000×) and unevenly distributed filamentous bundles were prominent features of tangutorine-treated cells (f, 4000×). Binucleated cells (k, 3750×) with multiple centrioles (l, 40,000×) were observed in cultures with a longer exposure of high doses of tangutorine (≥25 μg/ml) for 48 h, implicating aberrant mitosis occurred in cells.

scattered across the cell surface. The brush borders as well as the presence of tight junctions between neighboring cells are structural characteristics of intestinal epithelial cells [26]. Cells exposed to 25, 50, and 100 μg/ml tangutorine, however, had a dose-dependent decrease in the amount and length of microvilli on the surface of the cell (Fig. 4b and d). Many of the cells treated at 100 μg/ml tangutorine had a smoother, flattened surface with a loss of the uniform presence of microvilli, indicating that the cells were dead (Fig. 4d).

Untreated cells going through mitosis rounded up and loosely attached to the tissue culture plates (Fig. 4c). Some mitotic cells still could be found in culture treated with 25 μg/ml tangutorine (Fig. 4b) while not many of these round cell pairs were observed in cells treated with 50 μg/ml tangutorine. Most of the cells were incompletely divided or dead at higher doses of tangutorine (e.g. ≥100 μg/ml).

Transmission electron micrographs of HT29 cells showed that all untreated and tangutorine-treated cells had intact plasma membranes that still held all the contents of the cell within its boundaries (Fig. 4e and f). Normal HT29 cells were characterized by having microvilli, microfilaments, large mitochondria, smooth and rough endoplasmic reticulum with free ribosomes, lipid droplets, and very few primary lysosomes and many secondary lysosomes (Fig. 4g and i) [27]. Upon treatment with tangutorine, lysosomes appeared to have larger diameters but were still found scattered throughout the cytoplasm like untreated cells (Fig. 4f). Residual bodies with ''whorls of membranes'' and vacuolization were most clearly captured in cells treated with ≥75 μg/ml of tangutorine (Fig. 4f). The number of vacuoles increased in a dose-dependent manner, particularly at 100 μg/ml of tangutorine.

Alterations in cell shape by tangutorine may be due to changes of the intracellular cytoskeleton (Fig. 4j). The loss of the stretched out morphology associated with HT29 cells appears to be correlated with components involved in the cytoskeleton (microfilaments, microtubules, or intermediate filaments). Untreated HT29 cells had elongated filaments loosely bundled together sitting in an organized fashion located near the nucleus and mitochondria in the cytoplasm of the cell (Fig. 4i). In treated cells, filaments were densely bunched together in a chaotic fashion (Fig. 4j). Binucleated cells with several centrioles (Fig. 4k and l) were observed in cultures exposed to 12.5 μg/ml tangutorine for more than one cell cycle (48 h), indicating polyploidy cells were a result of mitotic slippage of HT29 cells.

Mitochondria in untreated HT29 cells appeared as elongate or oblong-shaped entities scattered throughout the cytoplasm as shown in the control HT29 cells (Fig. 4g). The mitochondria in untreated HT29 cell populations reflected the known descriptions of mitochondria by having a well-defined inner and outer membrane, matrix, intermembranous space, and most importantly the cristae. Cristae in untreated HT29 cells were arranged like a series of layers, tightly packed and shelf-like without the appearance of large areas of matrix. However, in HT29 treated with >50 μg/ml tangutorine the amount of cristae inside the mitochondria decreased and was pushed to one end of the organelle creating a dumbbell-like shape (Fig. 4h). Mitochondria also appeared swollen and larger than those of untreated cells. In some cases this enlargement of the mitochondria is referred to as megamitochondria [28]. The cristae within the mitochondria were more spaced out losing the shelf-like consistency of the cristae in the untreated cells. Nuclear morphology typical for apoptosis, e.g. condensation and margination of chromatin, was not observed in tangutorine-treated cells.

3.3. Dose-dependent flow cytometric analysis

In order to investigate if there was a dose-dependent effect of tangutorine on the cell cycle, cells were treated with 0, 3.125, 6.25, 12.5, 25, 50, 75, 100 and 150 μg/ml tangutorine for 24 h. Serum starvation yielded cell distributions of 80% of cells at G0/G1, 5% at S, and 11% at G2/M phase as shown in Fig. 5. Results show a dose specific accumulation of cells in different phases of the cell cycle, 3.125–12.5 μg/ml for G2/M phase (about 45% cells at 6.25 μg/ml), 6.25–25 μg/ml for S phase (about 46% at 25 μg/ml) and 25–100 μg/ml for G1 phase of the cell cycle (84% at 75 μg/ml) (Fig. 5b). The progressive increase of G2/M cells coincided with the increase of cell proliferation and cell counts at low doses of tangutorine treatment (Fig. 2a and b), however, cells could not cross the S-G2/M and G1-S transition in a dose-dependent manner, and underwent evident cell cycle arrest at S and G1 phases, respectively. DNA fragmentation became prominent at 100 μg/ml with a concurrent decrease of G1 cells, indicative of cell death. The distributions of HT29 cells through the cell cycle were modified differently depending on the concentration of tangutorine used. Since 50 μg/ml tangutorine induced a dramatic cell arrest in HT29 cells, prompting us to analyze a tangutorine-mediated kinetic change of HT-29 for 48 h.

3.4. Time-dependent flow cytometric analysis

Approximately 85% of HT29 cells were synchronized at the G0/G1 threshold phase of the cell cycle at 0 h and stimulated to re-enter the cell cycle by releasing into RPMI medium containing 10% FBS or a combination of serum and 50 μg/ml of tangutorine for the treatment group (Fig. 6). The results show that drug treatment triggered a cell cycle arrest at the G1 to S boundary. Cell cycle perturbations caused by tangutorine were not evident from between 0 to 12 h, during which both treated and untreated cell populations aggregated in the G1 phase preparing to move into the S phase. Starting from 15 h, treated cells

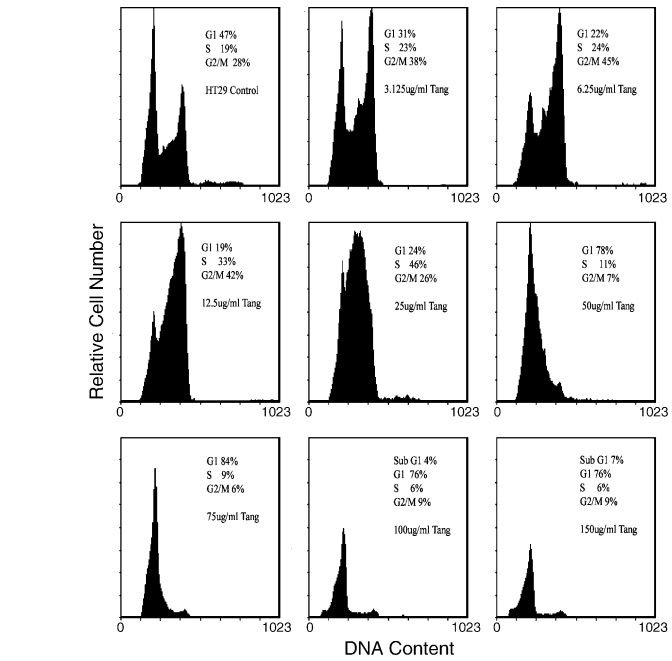

(a) **DNA pattern of Tangutorine-treated HT29 cells**

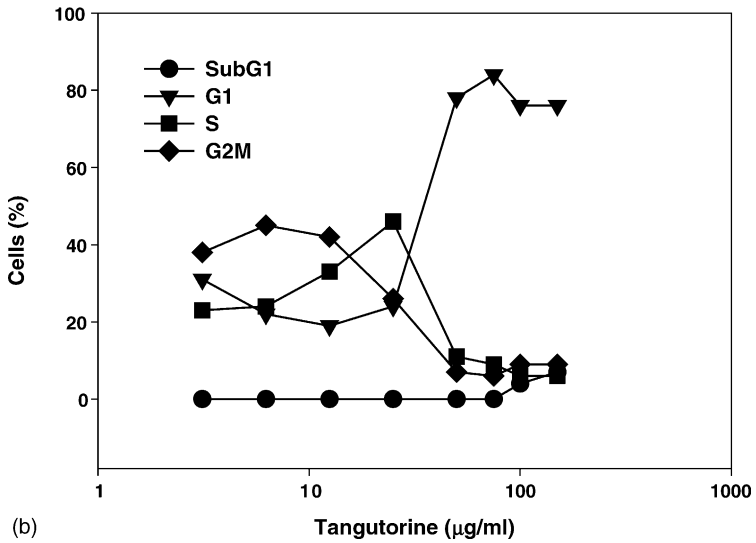

(b)

Fig. 5. A diverse dose-specific cell cycle regulatory activity of tangutorine on HT29 cells as demonstrated by flow cytometry. More cells accumulated in G2M phase at doses 3.125–12.5 μg/ml tangutorine, S phase at 6.25–25 μg/ml, and G1 phase at 25–100 μg/ml (a). DNA fragmentation became obvious in cells treated with 50 μg/ml or above of tangutorine for 24 h (b).

were delayed from progressing from G1 (78%) into the S phase (13%) of the cell cycle while a large proportion of untreated cells were progressing from the late G1 (78% at 12 h to 56% at 15 h) of the cell cycle into S (27% at 15 h). The increase in cell distributions in S and G2/M were linked to a simultaneous decrease in the number of cells in the G1 phase most noticeably for the control cells. By 21 h, the accumulation of cells in the S phase of treated cells is even more apparent at 35% compared to the 15% in untreated samples. About 50% of cells progressed from G2M phase at 21 h and finished the cell cycle at about 24 h with about 50% cells had already entered G1 phase of the second cell cycle. No significant increase of G2/M cells can be noted in the treated samples with significant decrease of G1 cells, indicating the delayed entry into the G2/M phase between 18 and 27 h of treatment with tangutorine.

From the period between 24 and 48 h the untreated cells go through another round of division while treated cells started to decrease in number. The majority of treated cells seemed fully incapable of passing through both the S and

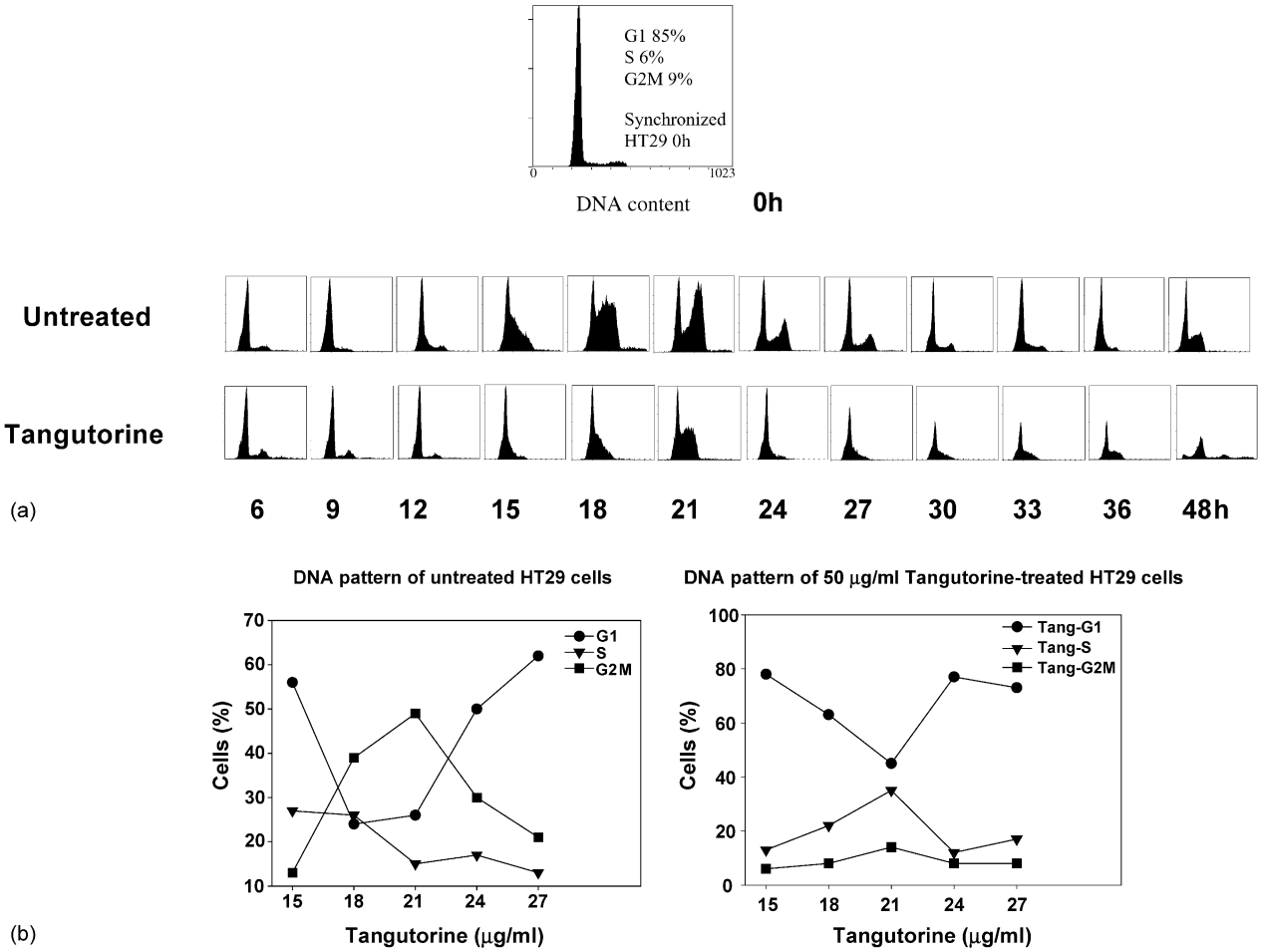

Fig. 6. Kinetic effects of tangutorine (50 μg/ml) on cell cycle distribution in HT29 cells. Cells were synchronized by serum depletion for 48 h (85% G1 cells) before they were treated with 50 μg/ml tangutorine (a). DNA replication (S phase) is around 15–21 h and mitosis at 21–24 h in untreated cells before they started another cell cycle at around 27 h. A delay of S phase (15–18 h) and a lower G2M phase (14% vs. 49% for treated and untreated cells, respectively) were measured in treated cells. More than 80% cells arrested in G1 phase and did not proceed into a second cell cycle even up to 48 h, but about 5% of cells expressing 8 N, implicating some cells slipped through G2M arrest and formed aberrant mitosis (b).

G2/M phases and had arrested in the G1 phase of the cell cycle.

3.5. Expression of cell cycle regulatory proteins

Fig. 7 shows the western blotting results for the expression of cell cycle related proteins cyclin B, cdc2, cyclin D, cdk4, cdc25, p21, and topoisomerase II after 24 h treatment with various concentrations of tangutorine. With respect to the control, tangutorine treatment up-regulated G2 regulatory proteins, such as cyclin B, cdc2 and cdc25, before they dropped abruptly between 12.5 and 50 μg/ml tangutorine (Fig. 7a), which may attribute to the proliferative activity of tangutorine at $\leq$12.5 μg/ml, as demonstrated by MTT assay and trypan blue exclusion count (Fig. 2a and b). The level of proliferating cell nuclear antigen (PCNA, the auxiliary protein of DNA polymerase) remained steadily regardless of treatment doses of tangutorine, but its function in DNA replication was likely inhibited by a significant increase of cyclin kinase inhibitor p21 from 12.5 to 50 μg/ml tangutorine (Fig. 7a). This p21 increase was independent of the status of its upstream cyclin kinase inhibitor p53 because HT29 cells have mutant p53 protein [27]. The expression level of topoisomerase II protein, a nuclear enzyme regulating the topological states of DNA during replication [29], was up-regulated in a dose-dependent manner before it declined most evidently at 12.5 μg/ml tangutorine (Fig. 7b).

3.6. Reverse transcription-polymerase chain reaction analysis

Depending on the dosage, treatment of tangutorine for 24 h up-regulated transcriptional expression of p21 gene in HT29 cells (Fig. 8). Expression of p21 mRNA was at an undetectable level in the untreated cells and increased in cells treated with 50 μg/ml tangutorine and dropped

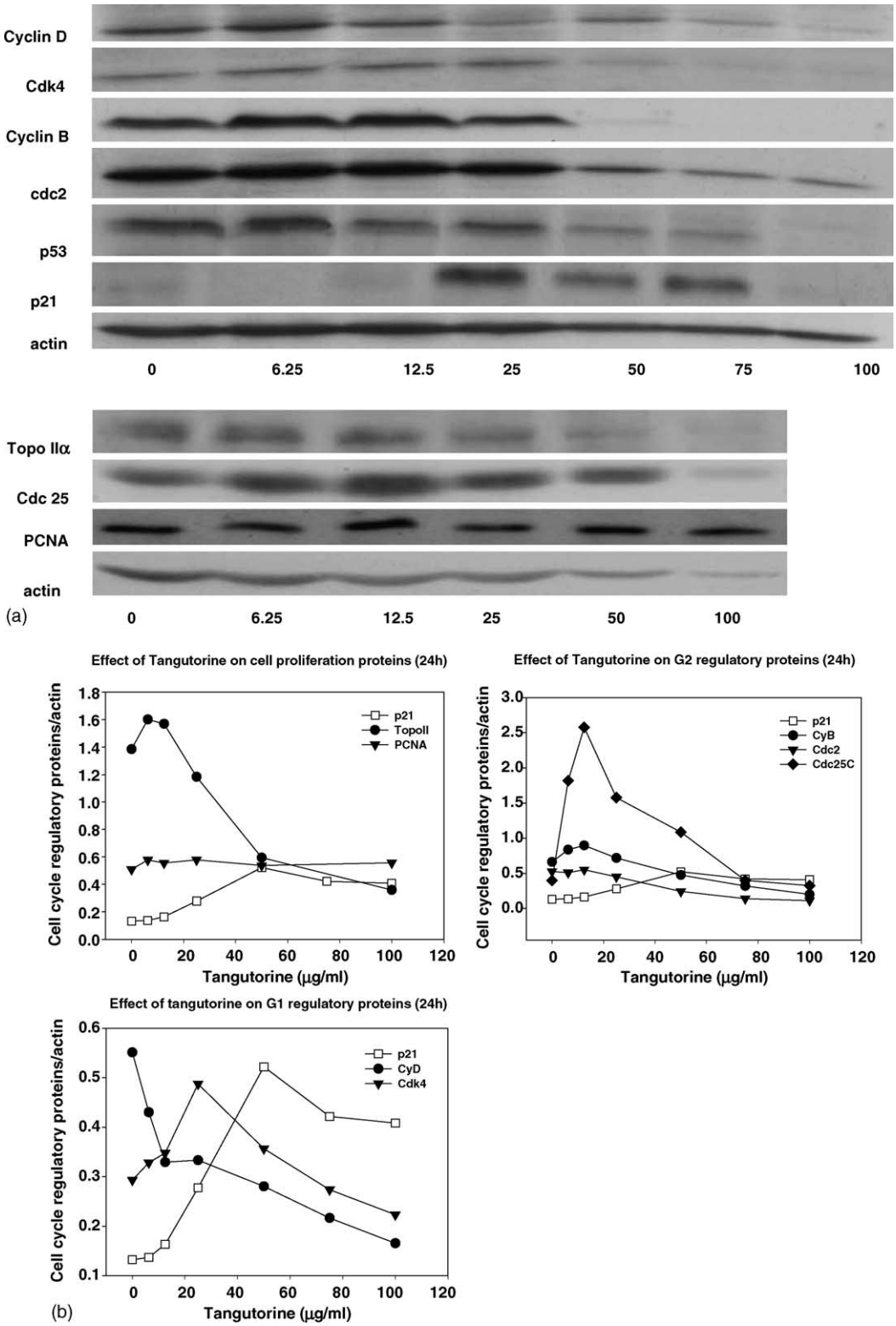

Fig. 7. Analysis of cell cycle regulatory proteins by immunoblotting analysis (a). A significant decrease of topoisomerase II, cyclins (B and D) and cyclin kinases (cdk4 and cdc2) in cells at doses higher than 25 μg/ml at the concurrent increase of cyclin kinase inhibitor p21. This p21 increase is independent of the status of cyclin kinase inhibitor p53 because p53 protein is mutated in HT29 cells. PCNA remained unchanged irrespective to any tangutorine treatment (b).

abruptly thereafter. p21 mRNA expression was back to very low levels after treatment with 100 μg/ml tangutorine for 24 h (0.4 versus 0.07 for 50 and 100 μg/ml, respectively).

4. Discussion

Two assays, MTT assay and trypan blue exclusion count, were used to assess the cytotoxicity of tangutorine on

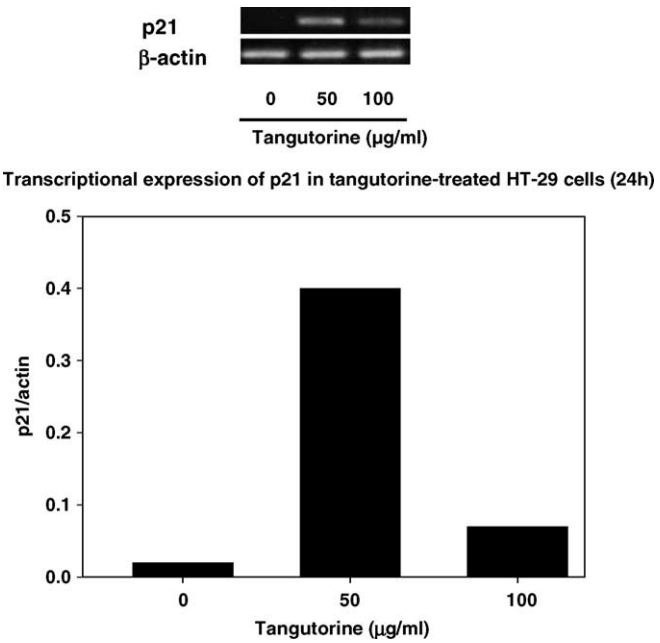

Fig. 8. Effect of tangutorine for 24 h on the transcription of p21 in HT29 cells. p21 mRNA was at an undetectable level in the untreated cells and increased in samples extracted from cells treated with 50 μg/ml tangutorine and declined thereafter.

human colon cancer HT-29 cells. The results of the MTT assay are consistent with the cell count assay; in both tests, a slight stimulatory activity on HT-29 cells at low doses of tangutorine ($\leq$12.5 μg/ml) but markedly suppressed DNA synthesis at concentrations between 25 and 50 μg/ml from 24 to 48 h. Increasing the tangutorine incubation period 24 h at these two concentrations increased cytotoxicity at 43–45%. On a dose-related scale, the most dramatic increases in cytotoxicity occurred at >100 μg/ml tangutorine when most probably cells died (Fig. 2).

Morphological examination showed that extra- and intra-cellular structures were profoundly affected after treatment with tangutorine in a dose-dependent manner. Extracellularly, tangutorine-treated cells had increasingly shorter microvilli that progressively disappeared in a dose-dependent manner. Cells were also characterized with a loss of the elongated morphology to a more rounded-up state. It is believed that tangutorine induced these morphological alterations on HT29 cells through rearrangements of the cytoskeleton similar to taxol, colchicines, Vinca and the β-carboline alkaloids [18,30]. Incomplete cell division was observed in HT29 cells after treatment with higher doses of tangutorine (Fig. 4), implicating that cells had passed S phase but failed to progress through mitosis of the cell cycle because of the down-regulation of G2M regulatory proteins (Fig. 7). However, some cells did escape from prolonged mitotic arrest and resulted in polyploidy G1 cells with multiple nuclei [18,31,32] and centrioles [33], which were also observed in HT29 cells treated with 12.5 μg/ml tangutorine for 44 h (more than one cell cycle), strongly demonstrating a mitotic slippage of these cells in the present experiment. Experiments with p21- and p53-deficient cells are being conducted to elucidate the role of these kinase inhibitors in this aberrant mitosis.

Tangutorine-treated cells had increased swollen mitochondria with altered internal structures as well as hypervacuolization in a dose-dependent manner. The swelling and enlarged mitochondria are believed to be a morphological transition that occurs prior to cell death or part of the physiological cell death process in response to a variety of stimuli [28,34]. In the present study the formation of swollen mitochondria did not appear to be linked to apoptosis because fragmentation of cells into apoptotic bodies, chromatin condensation, swelling of the endoplasmic reticulum or Golgi apparatus, and cell shrinkage, the characteristic features of cells undergoing apoptosis [24,35,36] were not observed by light, fluorescence, and electron microscopic analysis of tangutorine-treated cells. Instead of the increasing formation of vacuoles in tangutorine treated cells that may be a process occurred in the cell upon exposure to a cytotoxic agent, such as fibroblasts treated with wheat germ lectin [23].

Results obtained from flow cytometry and immunoblotting suggest that different concentrations of tangutorine were quite effective in inducing a deregulation of HT29 cell proliferation through modulation of cell cycle regulatory proteins. HT29 cells treated with a serial concentrations of tangutorine for 24 h gave sufficient exposure time to the drug, which elicited multi-phase cell cycle arrest depending on the concentration used. A kinetic study done on HT29 cells treated with 50 μg/ml tangutorine throughout a 48 h period stems from the fact that p21 protein expression was up-regulated modestly until a dramatic increase between 25 and 50 μg/ml tangutorine and dropped thereafter (Fig. 7). As shown in the ^{3}H-Tdr incorporation experiments, DNA synthesis was inhibited in a dose-dependent manner, most dramatically at concentrations of tangutorine at 25 μg/ml and greater. Its expression induced a S-phase arrest at 25 μg/ml and G1 arrest at $\geq$50 μg/ml either by associating to CDK–cyclin complexes [36,37], by binding to PCNA for inhibition of DNA synthesis [38,39] or interfering with the catalytic activity of topoisomerase II for normal mitosis [40] throughout the 48 h period. PCNA has unlikely played an active role in the inhibitory activity of tangutorine in this study because its levels in HT-29 cells remained relatively stable regardless of tangutorine concentration (Fig. 7). However, up-regulation of p21 and a decrease in the protein levels of topoisomerase II, cyclin B and cdc2 (Fig. 7) inhibited the S-G2M transition [41,42], accounting for a S-arrest or an incomplete mitosis. The increasing doses of tangutorine ($\geq$25 μg/ml) not only maintained a high level of p21, but also down-regulated the protein levels of all Cdk (cdc2 and cdc25C), cyclins (D and B), and topoisomerase II that are necessary for the progression of the cell through the cell cycle. Cells accumulated at G1

phase before they died without any evidence of apoptosis as analyzed by both fluorescence and transmission electron microscopy [43–45].

Cyclin B and cdc2 are intricately involved in the progression of the cell cycle through the G2/M phase transition [41,42]. The coupled decrease of cyclin B and cdc2 levels along with the induction of p21 can also cause cell cycle arrest are usually associated with an arrest in the G2/M transition of the cell cycle [46]. The distribution of cells in the S and G2/M during 21 h shows that perhaps the expression of p21 must reach an optimum level during or after 24 h in order to investigate a stable arrest in the G1. The movement of cells into S phase is visibly delayed from entry into S phase starting from 15 to 21 h as compared to the control. Some cells visibly start DNA synthesis, as suggested by the increase of cells in the S phase from 15 to 21 h, but fail to complete DNA replication upon entry into G2/M at 21 h. It seems that presence of unreplicated DNA in G2/M triggers the activation of the G2/M checkpoint which leads to the down-regulation of cyclin B, cdc2, cdc25c, and topoisomerase II by 24 h as shown by the immunoblotting results. Biparametric analysis of immunofluorescence of p21 versus the regulatory proteins were not used in this study due to limitations imposed by the intrinsic autofluorescent properties of tangutorine at concentrations $\leq$100 μg/ml which did not pose interference in the red fluorescent dye for cell cycle analysis, determined by the reproducibility and stability of the results obtained.

p21 is also known for its ability to be up-regulated by the tumor suppressor gene p53, both of which are integrated in G1 and G2 arrest machinery in response to DNA damage [31,47]. The results of this study suggest that the mechanism of action through which tangutorine up-regulates p21 expression is through a p53-independent pathway. Treatment of HT29 cells with tangutorine robustly inhibited the expression of the tumor suppressor protein p53. In studies where p53 induces the expression of p21 for cell cycle arrest, p53 expression levels are up-regulated in parallel with the increased expression of p21 [47]. The wild type p53 gene has been identified to be a major regulator of apoptosis and the cell cycle progression [41], but is non-functional in HT29 cell lines due to a mutation in the p53 gene [27]. Coradini and colleagues [44] showed that p53 was in fact mutated in the HT29 cell line through sequencing analysis and found that cell cycle arrest could still be induced by sodium butyrate through an up-regulation of p21 even though there was a down-regulation in p53 expression [44]. This is also in accordance to other studies with cell cycle arrest in the presence of mutated p53 genes where p21 expression was regulated by p53-independent mechanisms in response to the isoflavone genistein [46] and alkylphospholipids [48].

The expression of topoisomerase II mRNA increases in the late S and G2/M phases of the cell cycle indicating the importance of its activity in helping cells go through the final stages of cell division [40]. The immunoblotting assays on topoisomerase II showed that there was a dose-dependent decrease of topoisomerase II protein expression in tangutorine treated HT29 cells. The decrease in topoisomerase II can also be indicative of topoisomerase II inhibitory effects of tangutorine like in tangutorine-treated LNCaP (unpublished data). The characteristic cytotoxic effects that can be caused by topoisomerase II inhibitors like etoposide, genistein and harmine involve an arrest of cells at the G2/M transition [46,49,50]. Topoisomerase II poisons, such as camptothecins, can also cause DNA damage in the S phase which leads to either a S phase or G2 phase arrest [51]. Topoisomerase II protein expression starts to drop at 25 μg/ml, in parallel with an S phase arrest. At lower concentrations of tangutorine ranging from around 6.25 to 12.5 μg/ml, it appears that cells have arrested in the G2/M. However, it does not appear that the G2/M arrest is associated with topoisomerase II inhibition because protein expression was not shown to drop until 25 μg/ml tangutorine. It cannot be ruled out that the decrease in topoisomerase II did not have any effect in triggering the activation of the G2 topoisomerase II-dependent checkpoint in response to the inability to condense and segregate chromosomes since aneuploidy or polyploidy are characteristic of topoisomerase II inhibitors [49]. In summary, we have demonstrated a broad spectrum bioactivities of tangutorine, a β-carboline with unique chemical structure isolated from the leaves of *Nitraria tangutorum*, on colon cancer HT29 cells, providing an insight into the molecular mechanisms.

Acknowledgments

The authors would like to thank Ms. J. Hou and Mr. S.C.W. Sze for technical assistance.

References

[1] Duan JA, Williams ID, Che CT, Zhou RH, Zhao RH. Tangutorine: a novel β-carboline alkaloid from *Nitraria tangutorum*. Tetrahedron Lett 1999;40:2593–6.
[2] Jemal A, Tiwari RC, Murray T, Ghafoor A, Samuels A, Ward E, et al. Cancer statistics. CA Cancer J Clin 2004;54:8–29.
[3] Hong Kong Cancer Registry (2000) Hospital Authority: Cancer Stat. Available at: http://www3.ha.org.hk/cancereg/data/2000.pdf. Accessed: June 2004.
[4] Armand JP, Ducreux M, Mahjoubi M, Abigerges D, Bugat R, Chabot G, et al. CPT-11 (irinotecan) in the treatment of colorectal cancer. Eur J Cancer 1995;31A:1283–7.
[5] Cvitkovic E, Bekradda M. Oxaliplatin: a new therapeutic option in colorectal cancer. Semin Oncol 1999;26:647–62.
[6] Guichard S, Cussac D, Hennebelle I, Bugat R, Canal P. Sequence-dependent activity of the Irinotecan-5FU combination in human colon-cancer model HT29 in vitro and in vivo. Int J Cancer 1997;73:729–34.
[7] Yu HG, Huang JA, Yang YN, Huang H, Luo HS, Yu JP, et al. The effects of acetylsalicylic acid on proliferation, apoptosis, and invasion

of cyclooxygenase-2 negative colon cancer cells. Eur J Clin Invest 2002;32:838–46.
[8] Hartwell LH, Kastan MB. Cell cycle control and cancer. Science 1994;266:1821–8.
[9] Xing SR. Ningxia Medicinal Flora, vol. 2. Ningxia, China: Ningxia People's Publishing House, 1991.
[10] Berner M, Tolvanen A, Jokela R. Synthesis of the tangutorine skeleton. Tetrahedron Lett 1999;40:7119–22.
[11] Luo S, Zificsak CA, Hsung RP. Intramolecular formal aza-[3 + 3] cycloaddition approach to indoloquinolizidine alkaloids. A stereoselective total synthesis of (±)-tangutorine. Org Lett 2003;5:4709–12.
[12] Putkonen T, Tolvanen A, Jokela R. First total synthesis of (±)-tangutorine. Tetrahedron Lett 2001;42:6593–4.
[13] Itoh T, Matsuya Y, Enomoto Y, Ohsawa A. A concise formal synthesis of (±)-deplancheine. Heterocycles 2001;55:1165–72.
[14] Birman VB, Rawal VH. A novel route to the Geissoschizine skeleton: The influence of ligands on the diastereoselectivity of the heck cyclization. Tetrahedron Lett 1998;29:7219–22.
[15] Deveau AM, Labroli MA, Dieckhaus CM, Barthen MT, Smith KS, Macdonald TL. The synthesis of amino-acid functionalized beta-carbolines as topoisomerase II inhibitors. Bioorg Med Chem Lett 2001;11:1251–5.
[16] Kawato Y, Aonuma M, Hirota Y, Kuga H, Sato K. Intracellular roles of SN-38, a metabolite of the camptothecin derivative CPT-11, in the antitumor effect of CPT-11. Cancer Res 1991;51:4187–91.
[17] Robinson ML, Martin BA, Gootz TD, McGuirk PR, Moynihan JA, Sutcliffe JA, et al. Effects of quinolone derivatives on eukaryotic topoisomerase II. A novel mechanism for enhancement of enzyme-mediated DNA cleavage. J Biol Chem 1991;266:14585–92.
[18] Tu LC, Chou CK, Chen CY, Chang YC, Shen YC, Yeh SF. Characterization of the cytotoxic mechanism of Mana-Hox, an analog of manzamine alkaloids. Biochim Biophys Acta 2004;1672:148–56.
[19] Uezono T, Maruyama W, Matsubara K, Naoi M, Shimizu K, Saito O, et al. Norharman, an indoleamine-derived β-carboline, but not Trp-P-2, a γ-carboline, induces apoptotic cell death in human neuroblastoma SH-SY5Y cells. J Neural Transm 2001;108:943–53.
[20] Song Y, Kesuma D, Wang J, Deng Y, Duan J, Wang JH, et al. Specific inhibition of cyclin-dependent kinases and cell proliferation by harmine. Biochem Biophys Res Commun 2004;317:128–32.
[21] Davis PK, Ho A, Dowdy SF. Biological methods for cell-cycle synchronization of mammalian cells. BioTechniques 2001;30:1322–31.
[22] Ho JCK, Sze SCW, Shen WZ, Liu WK. Mitogenic activity of edible mushroom lectins. Biochim Biophys Acta 2004;1671:9–17.
[23] Liu WK, Sze SCW, Ho JCK, Liu BPL, Yu MC. Wheat germ lectin induces G2/M arrest in mouse L929 fibroblasts. J Cell Biochem 2004;91:1159–73.
[24] Liu WK, Xu SX, Che CT. Anti-proliferative effect of ginseng saponins on human prostate cancer cell line. Life Sci 2000;67:1297–306.
[25] Sze SCW, Ho JCK, Liu WK. *Volvariella volvacea* lectin activates mouse T lymphocytes by a calcium dependent pathway. J Cell Biochem 2004;92:1193–202.
[26] Cohen E, Ophir I, Shaul YB. Induced differentiation in HT29, a human colon adenocarcinoma cell line. J Cell Sci 1999;112:2657–66.
[27] Fogh J, Trempe G. In: Fogh J, editor. Human Tumor Cells In Vitro. New York: Plenum Press; 1975. p. 115–59.
[28] Wakabayashi T, Karbowski M. Structural changes of mitochondria related to apoptosis. Biol Signals Recept 2001;10:26–56.
[29] Dassonneville L, Lansiaux A, Wattelet A, Wattez N, Mahieu C, van Miert N, et al. Cytotoxicity and cell cycle effects of the plant alkaloids cryptolepine and neocryptolepine: relation to drug-induced apoptosis. Eur J Pharmacol 2000;409:8–18.
[30] Lobert S, Vulevic B, Correia JJ. Interaction of *Vinca* alkaloids with tubulin: a comparison of vinblastine, vincristine, and vinorelbine. Biochemistry 1996;35:6806–14.
[31] Andreassen PR, Lacroix FB, Lohez OD, Margolis RL. Neither $p21^{WAF1}$ nor 14-3-3σ prevents G2 progression to mitotic catastrophe in human colon carcinoma cells after DNA damage, but $p21^{WAF1}$ induces stable G1 arrest in resulting tetraploid cells. Cancer Res 2001;61:7660–8.
[32] Chen JG, Yang CP, Cammer M, Horwitz SB. Gene expression and mitotic exit induced by microtubule-stabilizing drugs. Cancer Res 2003;63:7891–9.
[33] Fernandez C, Lobo Md Mdel V, Gomez-Coronado D, Lasuncion MA. Cholesterol is essential for mitosis progression and its deficiency induces polyploid cell formation. Exp Cell Res 2004;300:109–20.
[34] Petit PX, Lecoeur H, Zorn E, Dauguet C, Mignotte B, Gougeon ML. Alterations in mitochondrial structure and function are early evens of dexamethasone-induced thymocye apoptosis. J Cell Biol 1995;130:157–67.
[35] Boe R, Gjertsen BT, Vintermyr OK, Houge G, Lanotte M, Doskeland SO. The protein phosphatase inhibitor okadaic acid induces morphological changes typical of apoptosis in mammalian cells. Exp Cell Res 1991;195:237–46.
[36] Faa G, Ledda-Columbano GM, Ambu R, Congiu T, Coni P, Riva A, et al. An electron microscopic study of apoptosis induced by cyclohexamide. Liver 1994;14:270–8.
[37] Xiong Y, Hannon GJ, Zhang H, Casso D, Kobayashi R, Beach D. p21 is a universal inhibitor of cyclin kinases. Nature 1993;366:701–4.
[38] Cayrol C, Knibiehler M, Ducommun B. p21 binding to PCNA causes G1 and G2 cell cycle arrest in p53-deficient cells. Oncogene 1998;16:311–20.
[39] Sekiguchi T, Hunter T. Induction of growth arrest and cell death by overexpression of the cyclin-Cdk inhibitor p21 in hamster BHK21 cells. Oncogene 1998;16:369–80.
[40] Cortés F, Pastor N, Mateos S, Dominguez I. Roles of DNA topoisomerases in chromosome segregation and mitosis. Mut Res 2003;543:59–66.
[41] Knockaert M, Greengard P, Meijer L. Pharmacological inhibitors of cyclin-dependent kinases. Trends Pharmacol Sci 2002;23:417–25.
[42] Shah MA, Schwartz GK. Cell cycle-mediated drug resistance: an emerging concept in cancer therapy. Clin Cancer Res 2001;7:2168–81.
[43] Barnouin K, Dubuisson ML, Child ES, Fernandez de Mattos S, Glassford J, Medema RH, et al. H_2O_2 induces a transient multi-phase cell cycle arrest in mouse fibroblasts through modulating cyclin D and $p21^{Cip1}$ expression. J Biol Chem 2002;277:13761–70.
[44] Coradini D, Pellizzaro C, Marimpietri D, Abolafio G, Daidone MG. Sodium butyrate modulates cell cycle-related proteins in HT29 human colonic adneocarcinoma cells. Cell Prolif 2000;33:139–46.
[45] Wolter F, Akoglu B, Clausnitzer A, Stein J. Down-regulation of the cyclin D1/cdk4 complex occurs during resveratrol-induced cell cycle arrest in colon cancer cell lines. J Nutr 2001;131:2197–203.
[46] Choi YH, Lee WH, Park KY, Zhang L. p53-independent induction of p21 (WAF1/CIP1), reduction of cyclin B1 and G2/M arrest by the isoflavone genistein in human prostate carcinoma cells. Jpn J Cancer Res 2000;91:164–73.
[47] El-Deiry WS, Tokino T, Velculescu VE, Levy DB, Parson R, Trent JM, et al. WAF1, a potential mediator of p53 tumor suppression. Cell 1993;75:817–25.
[48] Patel V, Lahusen T, Sy T, Sausville EA, Gutkind JS, Senderowicz AM. Perifosine, a novel alkyphospholipid, induces $p21^{WAF1}$ expression in squamous carcinoma cells through a p53-independent pathway, leading to loss in cyclin-dependent kinase activity and cell cycle arrest. Cancer Res 2002;62:1401–9.
[49] Downes CS, Clarke DJ, Mullinger AM, Gimenez-Abian JF, Creighton AM, Johnson RT. A topoisomerase II-dependent G2 cycle checkpoint in mammalian cells. Nature 1994;372:467–70.
[50] Hande KR. Etoposide: Four decades of development of a topoisomerase II inhibitor. Eur J Cancer 1998;34:1514–21.
[51] Cliby WA, Lewis KA, Lilly KK, Kaufmann SH. S phase G2 arrests induced by topoisomerase I poisons are dependent on ATR kinase function. J Biol Chem 2002;277:1599–606.